J. Condensed Matter Nucl. Sci. 6 (2012) 1–12

Research Article

When Bubble Cavitation becomes Sonofusion

Roger S. Stringham *

First Gate Energies, PO Box 1230, Kilauea, HI 96754, USA

Abstract

Experimentally, excess heat, *Qx*, and ^{4}He are the measured fusion products of transient high-density sonofusion, SF. A possible path to DD fusion is explained by piezo driven cavitation bubbles, where the critical parameters are temperature, pressure, acoustic input, and frequency that control, for a picosecond, the low-energy nuclear reactions that produce DD fusion events. The electromagnetic, EM, pulse compressed deuteron clusters squeezing them into a Bose Einstein Condensate. The BEC cluster environment provides for the direct conversion of fusion energy into heat and ^{4}He. The continuous production of 10^{16} bubbles/sec produces radiation free usable heat as observed via ejecta site surveys.

Keywords: BEC, Charged-plasma, Clusters, High-density, Sonofusion

1. Introduction

The high transient density of inertial confined fusion, ICF [1,2] along with new astrophysical information and the ultra low-temperature bosons and fermions [3] are linked and can be applied to a sonofusion, SF, model by way of sub-nanometer deuteron clusters. The SF cluster systems are 1000 times faster and 10^{18} times smaller in volume, m^3, and number of particles than the hot fusion ICF systems [4]. The SF model is a series of sequential steps where the cavitation and jet are already well established in mainstream science. The formation of transient clusters and their compression is more speculative. The determination of a heat source from ejecta site data is the logical interpretation of scanning electron microscopy, SEM, photos of ejecta site surveys on exposed target foils [5]. The products measured are ^{4}He and heat via mass spectroscopy and calorimetry. A tentative explanation of a path to the produced fusion products of heat, *Qx*, and ^{4}He needed an explanation with the association of the collapsing bubble, the jet, the sonofusion deuteron cluster, the heat pulse, and the ejecta site [4,6].

2. Sonofusion Process

Some of the basic information on the well-documented cavitation processes that produce very high transient energy densities is reviewed [7]. Cavitation is known to be a destructive force but in sonofusion this force is turned around

*E-mail: firstgate@earthlink.net

to produce useful heat in a transient DD fusion environment via transient cavitation bubbles, TCBs, in circulating D_2O. A resonating piezo is the source of the sonofusion driven acoustic power. The feedback oscillator driven piezos produce a variable size bubble population where the natural individual resonance properties of a bubble couple with the parameters of pressure, temperature, and acoustic power of the cavitating D_2O. In recent years at higher frequencies of 1600 kHz, piezo resonance reduces the damage characteristics found using lower frequencies. The initial bubble passes through phases in a microsecound where its resonant radius of about 0.2 μm grows isothermally gaining mass and size to a maximum radius of about 2 μm immediately followed by its violent adiabatic collapse to its final radius of about 0.02 μm producing sonoluminescence, SL, and a high-density jet. At 1.6 MHz the volume increase in the one cc reactor volume of the D_2O will increase about 1%. This frequency will generation of 10^{10} of 4 μm diameter bubbles, maximum, in one acoustic cycle or 10^{16}/s. This number of bubbles has the potential of producing 10^{17} clusters/s and 10^5 W. Experimentally for a 40 W Qx the 1.6 MHz system is working at an efficiency of $40/10^5 = 0.0004$.

During its collapse, a tremendous increase in the bubble's energy density occurs where the external pressure controls the initial energy density in the circulating D_2O. An adiabatic bubble collapse shows a one-hundred-fold decrease in the bubble radius and leads to about a 10^6 increase in energy density. Ideally this is the case but surface oscillations and shock waves are a reality and dampen the bubble's energy density during one acoustic cycle. The high-density jet produced at collapse has a structure of exterior sheath electrons transferred from the bubble's interface. These high velocity electrons are involved in an EM z-pinch compression of the jet's contents. The jet implants dense a plasma of electrons and deuterons into a target foil that immediately separate. The deuterons cluster as an EM picosecond pulse produces a cooling and compressing environment for BEC fusion that producing Qx, heat, and ^{4}He.

3. Jet Formation and SL

The TCB bubble jet is formed by the violent implosion of the bubble in the cavitating D_2O acoustic field. The acceleration collapse process produces jets composed of dissociated D_2O, a partial plasma [4]. The jet's outer and inner surface is the stretched collapsing bubble surface, an electron sheath, enclosing a picosecond z-pinched deuteron plasma. The produced sonoluminescence has been used to monitor SF, and is a tool for looking at the plasma condition at that instant of photon emission measured with a photo-multiplier device. Managing the parameters of temperature, pressure, and acoustic input controls the plasma condition for a particular piezo frequency. The reactor sonoluminescence measurements relate the condition of implanting plasma into an accelerating projection of the bubble interface into the form of a jet. There are many more jets formed than are implanted into the target foil and there are other reactor geometries that may be superior, but for the present the ability to observe sonoluminescence with the disk configuration is necessary for control of sonofusion's intensity observation. Only those jets within a few μm of the target surface will implant. The transient change of the bubbles into jets has been photographed [5].

4. The Jet Squeeze of the High-Density Plasma Jet

The velocity of sheath electrons and the orientation of water's surface tension molecules provide for electromagnetic compression fields. The concentric layer model of the jet plasma and its high velocity sheath electrons make for a complex z-pinch of the jet's plasma contents and helps explain the jet's transient geometry. The jet is conical, construction consisting of a series of concentric layers starting with the outside water-deuteron interface, outer sheath electrons, the deuteron plasma, inner sheath electrons, and vacuum inner-core [4]. During the several picoseconds lifetime of the jet, it will implant the target foil before its natural z-pinch destruction. From the TCB metamorphosis, the jet's contents of deuterons and electrons are further compressed by electromagnetic, EM, pressures, via z-pinch forces, to higher densities in the order of 10^{32} D^+/m^3. The jet 20 Mach sheath electrons result from the final stage of the TCB [4] and the jet z-pinch. The total compression pressure's confinement of the jet contents is enhanced by

its passage through the cavitating D_2O dielectric. During this jet implantation the already dense plasma of the jet is further compressed. During this short time frame the jet will appear to be passing through a glass dielectric. The jet is on its way to a target implantation. The jet contents are implanted into the target foil lattice where the D^+ and e^- are momentarily separated.

5. Implantation and Cluster Formation

Figure 1 shows the deuteron cluster compression pulse just after the jet implant into the target foil. The impulse pressure of the Coulombically attracted cluster's free electrons produce a picosecond implosive EM pressure pulse that exceeds the cluster's repulsion relatively constant Coulombic escape pressure. Deuterons and electrons enter as an implanted dense plasma jet with the high impact velocity of a meteor, 30 k/s. At the point of jet impact into the target foil the jet implant energy is about equal to a single DD fusion event. Those electrons loosely associated with the higher energy levels of the deuterium atom were stripped of their remaining electron via lattice stripping and are part of the populations of separated deuterons and free mobile electrons. During the following femtoseconds the surrounding mobile electrons are directed via Coulombic implosive forces that clump deuterons into nm spheres, forming the deuteron cluster before Coulombic forces separate the D^+. The positive charge of the implanted deuterons attracts all surrounding free electrons to the cluster's center and can be compared with laser compressed 2 mm deuteron capsules, Inertial Confined Fusion [1]. During the picosecond EM compression pulse, the build up of compression heat is removed by cooling via evaporating surface deuterons of the BEC cluster contents. The energy of deuteron and electron recombination, 14.7 eV, occurs one nm away from the BEC cluster contents and produces a compression shock wave. The momentum exchange from the evaporation of cluster surface deuterons adds to the EM compression.

The BEC's high transition temperature, *Tc*, for clusters is based on its large energy gap between ε_0 and ε_1 that exist for the nuclear shell-model for deuterons in the picosecond EM pulse absence of electrons. Clusters cooled by evaporation should show a separation decrease associated with the de Broglie wave, λ_{Tc}, where a deuteron phase BEC may exist. D^+ at ε_0, the ground state, with the next energy level, with regard to its shell-model, of $\varepsilon_1 = 2.31$ MeV makes for a high *Tc* of millions of degrees for a picosecond for the cluster [8,9]. This is quite different from the electron shell energy level where one finds the next level above ground state about 0.06 eV.

The cluster is a squeezed BEC; for example, a 1 nm diameter of a million boson deuterium ions, or a smaller number, is cooled by the evaporation of its exterior cluster deuterons. In this example at 4000 K has a low T compared to the cluster's *Tc*. As the D–D cluster's separation decreases, the de Broglie wavelength over-lap increases. So the *T*/*Tc* ratio decreases improving the cluster's BEC character. It is important to keep the temperature, *T*, of the cluster low. The initial cluster radius of 0.5 nm is squeezed to 0.05 nm. There is a tendency for the cluster contents to heat as the cluster radius compresses to 0.1 radius. and the cluster volume approaches the density of muon fusion, 10^{36} D^+/m^3. The initial cluster density is 10^{30} to 10^{33} D^+/m^3. There is some evidence in Fig. 3(a) of super-dense transient clusters that fell through the Pd lattice target foil leaving gaping holes, perhaps initiated by tremendous transient cluster gravitational forces that broke out of the Pd lattice containment. A density of 10^{35} D^+/m^3 is 3.3×10^8 $kg/m^3$for a 1 nm cluster.

The Coulombic escape pressure of the cluster is much less than the implosive EM pressure pulse during the cluster's picosecond lifetime but is a constant force and after a picosecond the cluster will self-destruct through Coulombic repulsion pressures if no fusion occurs. The cluster coherence, superfluid properties, comes from the high-density low temperature of the cluster having a de Broglie deuteron wave much broader than the DD separation, 10^{-9} – 10^{-12} m, in the very dense cluster. The BEC nature of the cluster alters the path to the cluster's fusion event's products, which are heat, *Qx*, and ^{4}He with no gammas. If one compares muon fusion, MF, to SF, one finds the SF deutereron separation can be driven close to DD separation of MF. This path attempts to explain the products *Qx* and ^{4}He, sonofusion's experimental measured results. The difference is the ability of the SF BEC deuteron cluster to absorb the fusion heat pulse before any gamma can be produced. This fusion environment is the result of the cluster's BEC nature. The cluster

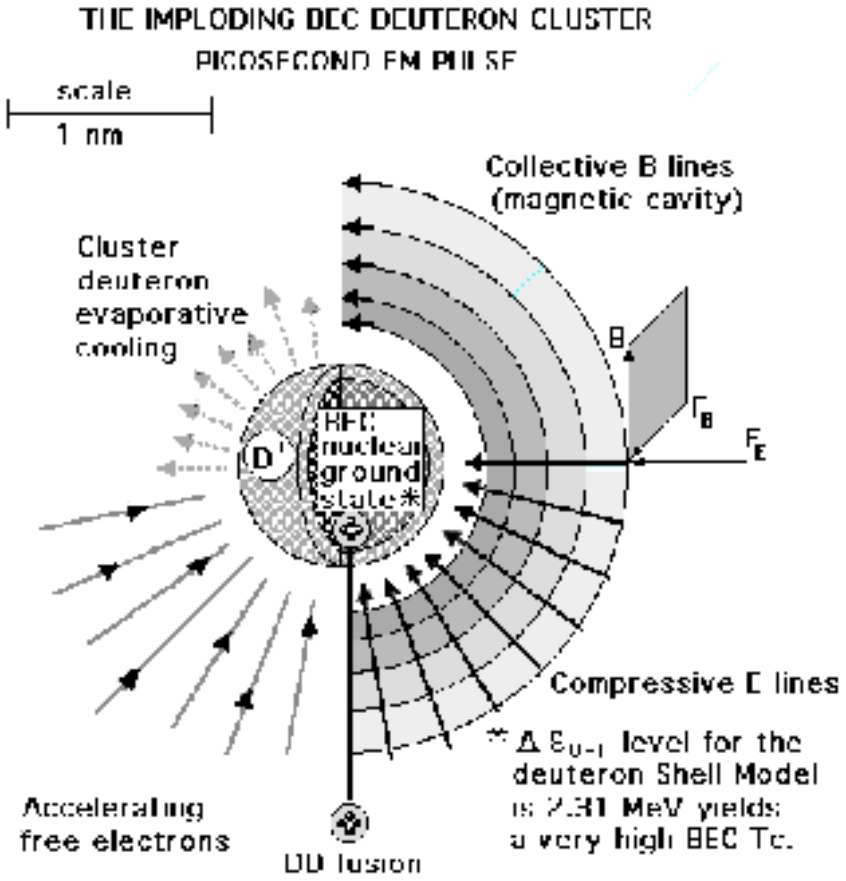

Figure 1. The spherical EM compressing *E* field and collapsing *B* field after the jet implantation creates a BEC D^+ cluster – a picosecond implosion pulse.

provides a large heat sink that immediately absorbs all the fusion *Qx* heat before other available paths such as the one oscillation required producing a 24 MeV gamma.

This is in contrast to muon fusion that has only two deuterons of mass, not enough to alter its fusion products of neutrons, gammas and helium, but can be viewed as a pseudo BEC phenomenon.

The implantation of jet electrons followed by deuterons produces clusters, schematically shown in Fig. 1. The figure shows a cluster with its EM compression pulse and the immediate neighborhood involving about a 3 nm volume with a 1 nm cluster volume. The clustered imploding picosecond EM pulse, divided into four over-lapping time phases, is shown during its BEC and fusion product formation. The one million deuteron clustered ions separation, 10^{-10} – 10^{-11}m, initial to a final diameter, 10^{-12-}m, is squeezed by an EM compression pulse [11]. The simultaneous aspects are: lower right the compressive *E* field lines, black arrows; lower left the accelerating free electrons, gray arrows; upper left the surface deuterons evaporating from the cluster surface cooling the BEC contents, broken arrows; the upper right shows the spherical containment of the *B* magnetic lines that squeeze the cluster, progressive gray spheres.

The black arrows show the EM implosion compressing pulse where the perpendicular 3D *E* field is a squeezing

pulse. The curved black arrows parallel to the cluster surface show the spherical magnetic 3D B field that forms the magnetic cavity of cluster containment during the EM picosecond cluster squeezing process. The evaporative cooling deuterons, the broken gray arrows in the upper left, remove heat from the cluster and eventually may recombine with some of the free accelerating electrons, away from the BEC contents. Electrons compress the cluster with their picosecond$E$field pressure pulse that exceeds the cluster's continuous Coulombic repulsion for a picosecond before D^+ repulsion or a fusion event destroys the cluster. The surrounding EM B and F_B are spherical, at right angles, and parallel to the cluster surface squeezing collectively as accelerating electrons advance to the surface, shown in Fig. 1. These self-generated B field lines contain the cluster in a magnetic cavity. The F_B force and B field are not enough to deflect the electrons on their short path to the cluster center. The curvature of the electron path, gray arrows, influenced by F_B of the accelerating electrons is minimal. During this picosecond the cluster of deuterons has been squeezed to a BEC superfluid shown as the dark dots representing D^+. The remaining interior deuterons are cooled by surface deuteron evaporation, one-half of the cluster's total deuterons, gray arrows, keep the BEC cool. Deuterons evaporated from the cluster's sphere surface may pick up an electron removing 14.7 eV away from the cluster. Fusion probably takes place near the cluster's surface, the four small spheres make an alpha. A spherical fusion heat pulse immediately fills the BEC, before any gamma formation, destroying the cluster and moving through the target lattice breaking the surface and escaping into the circulating D_2O releasing the Qx heat and helium four.

6. Experimental Results

6.1. Heat pulse

There have been more than twenty years of cavitation experiments coupled to fusion products heat and ^{4}He. It was determined, in the last 5 years, that the driving piezo resonant acoustic frequency shows a connection to the extent of cavitation damage via ejecta site size and distribution in target foils. The lower the frequency the greater the observed damage to the target foils. At high frequencies, 1.6 MHz, the ejecta sites remain small and are basically limited to one 20 MeV fusion event. The 1.6 MHz bubble systems involve much smaller numbers of deuterons, smaller jets, and smaller clusters. The ejecta site SEM photos of 1.6 MHz experiments show mostly single fusion events where the lower frequencies show both single and multiple fusion events. The population of these low-frequency multiple fusion events may be as high as 10^6 events. These large ejecta sites produce extensive damage to the target foils.

The frequency changes the acoustic input as to bubble size, and implantation, but not the energy density at the final stage of the bubble collapse as measured by sonoluminescence. The amount of energy that forms the ejecta site in the target foil is a function of the ejecta site diameter. Small area target foil surveys of ejecta site diameter population distribution of typically exposed target foils at different frequencies are shown in Figs. 2(a)–(c). Three frequencies were used in the experiments of sonofusion systems, 20, 46, and 1600 kHz (A–C). These had different ejecta size population distributions. See Figs. 2(a) and (c). These target foil ejecta site distributions are related to their energy by the diameter size (volume of ejecta) of each observed ejecta site. In this model the 50 nm diameter ejecta site equates to 20 ± 10 MeV as the ejecta site depth varies with the cluster deuteron implantation depth. The volume was calculated as the depth $2\times$ radius times the ejecta area. Of the three frequencies (A) at 20 kHz is the most destructive to the target foil. These ejecta sites had the highest bubble energy input, and produced the largest number of fusion events per cluster. The data for 20 kHz (A) systems was extrapolated from (B) and (C) population distributions because the SEM resolution at frequency (A) was low, around 0.3 μm. The damage at (A) was too low a resolution to do a proper survey. See Figs. 2(c) (A) and 3(a) and (b). Frequency, (B), at 46 kHz and 20 nm field emission SEM resolution showed, via survey, a decided decline in the severity of ejecta damage of exposed foils and showed fewer multiple fusion events per cluster than (A), but made up this discrepancy with an increase in the number of bubbles that formed implanting jets. Frequency of 1.6 MHz, (C), shows almost no visible damage except for a slight color change to the target surface. SEM photo of (C) and Fig. 5(a) and (b) shows many small single ejecta sites, about 50 nm in diameter, and few double sites.

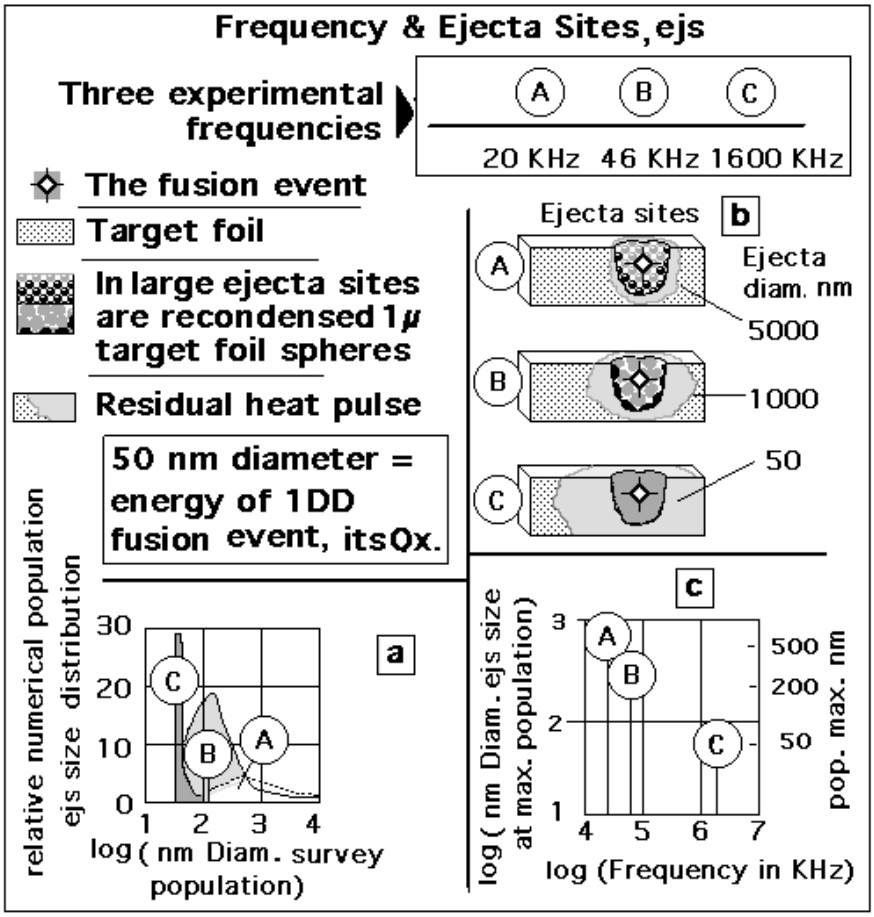

Figure 2. a, b, and c. The frequency influences the sizes of the cavitation bubble, the jet, the cluster, the heat pulse, and the ejecta sites. 2a is the ejecta site population distribution. 2b is the ejecta size. And 2c is the population distribution maximum. Ejecta volume is proportional to the cluster fusion events, single or multiple events.

At (C) the fusion event population was almost exclusively from single fusion events.

From surveys of the distribution of ejecta sites with respect to size (energy), Fig. 2(a), shows the dominance of small clusters at (C) resonance and their single fusion events. The lower resonance frequencies, (A) and (B), have fewer ejecta sites but show a majority of multiple fusion events.

Figure 2(b) shows the difference between the fusion energy in a single fusion event and multiple events originating in a cluster. The fact that the heat pulse ejects larger and more energetic clusters at lower frequency results in ejecta sites recondensed target foil spheres, 1 μm in diameter, in and around the heat pulse's ejecta site. The energy densities of (A)–(C) show sonoluminescence. The 50nm diameter ejecta site (C) shows a population almost entirely of single fusion event clusters. If the location of the cluster is too deep in the lattice, below the lattice surface, there may not be enough energy in the heat pulse to reach the target foil lattice surface. The Qx will be distributed in the foil where it is removed by the circulating D_2O. In this case a small amount of helium four will be captured in the lattice and will not

be collected as a gas for analysis. This helium is still in the foil and can be analyzed at a later date. The conditions, 1.6 MHz, of (C) make the Pd target much more suitable for commercial use. What (C) loses in number of fusion events per cluster it gains from the increased number of the much smaller transient cavitation bubbles and increased small cluster production in the target foil

Evidence of fusion events in Fig. 2(b) where ejecta volume of target foil vapors leaves behind 1 μm spheres of condensed Pd at the ejecta site at frequencies (A) and (B). The spheres are found imbedded on ejecta site walls and as free particles at the site. The target foils in the (C) system, 1.6 MHz, are free of the 1 μm particles as the particles are larger in diameter than the (C) ejecta site diameters. Note the residual heat pulse is distributed into the target foil lattice and remelts the adjacent lattice of earlier produced ejecta sites

Graph 2c for a given frequency shows that surveys of population of ejecta size diameters have a maximum number relating to cluster size. This population maximum size changes as the eject size distribution narrows with increasing frequency. The maximum ejecta size population is shown for each resonance frequency. The energy of the heat pulse from (A) and (B) destroys the target foil. In (C) there may not be enough energy to always break the surface of the foil. The foil may contain non-ejected ^{4}He as compared to a foil at (A) that shows little increase in ^{4}He residing in the target foil lattice as most is ejected into the D_2O. The magnitudes of chemical and nuclear events should be kept in mind.

6.2. Ejecta sites

Figures 3(a) and (b) are two SEM photos at 20 kHz (A) cavitation inputs exposing 100 μm thick Pd target foils to cavitating D_2O in Woodside Labratory, CA in 1993. The damage to this foil was extreme showing large ejecta events shown in SEM photos 3(a) and 3(b), where 10 μm ejecta site with loose 1 μm spheres were piled up inside its rim. See Fig. 2(c) (A). Figure 3(a) shows the general Pd surface terrain that needs to be resolved to make the ejecta survey count. A straight-line extrapolation of (B) and (C) in Fig. 2(c) is the maximum population number for (A).

Figures 4(a) and (b) are two field emission SEM photos at 46 kHz (B) with cavitation inputs exposing 100 μm thick 50 cm^2 Pd target foil, which includes both sides from a run at Stanford Research International, SRI. There have been many such foils and all show this type of ejecta damage at (B). Only a few exposed target foils have been analyzed via SEM photos. About 50% of the target foil surface in the sonofusion reactor comes in contact with the intense cavitation field that produces transient cavitation bubbles. The surface here is typical of the Pd target foil surfaces that have been photographed, and run at frequency (B). See Figs. 2(b) and (c) (B). Figure 4(c) shows the general Pd surface terrain that is expanded to about 1 square μm, 3d, for the ejecta survey count at 46 kHz exposed Pd target foil surface. This survey includes 21 ejecta sites with a wide distribution of ejecta site volumes.

Figures 5(a) and (b) are two FE SEM photos at 1600 kHz (C) with cavitation inputs exposing 100 μm thick Pd target foil from the First Gate lab in Kilauea, HI. The 1.6 MHz reactors were about 20 g compared to 5 kg for the 46 kHz devices. The one square μm of the field emission SEM photo 3(f) was surveyed and a total of 30 sites were found with a very narrow population distribution that consisted of 29 50 nm diameter sites, single fusion events, and one multiple ejection sites of two or three fusion events. This surface is much different showing no visual damage, only the very small events that appear not to lose target foil mass. See Fig. 2(c) (C). Figure 5(a) shows the general Pd surface terrain that shows the close packed 50 nm ejecta sites and survey count for the 1600 kHz, (C), exposed Pd target foil surface.

The SEM photos of sonofusion target foils exposed to cavitating D_2O at different acoustic driving frequencies are shown in Figs. 3–5. These are the same frequencies described for Figs. 2(a)–(c) and represent typical SEM analysis photos and survey counts of ejecta sites. Ejecta site survey distributions in small typical areas of exposed target foil are from SEM photos, Figs. 3(b), (4b), and (5b). The SEM photos of these figures correlate with Figs. 2(a)–(c). Figures 3(a) and (b) were SEM photos by John Dash at Portland State University. The other SEM photos taken by Jane Wheeler of Charles Evans lab in Sunnyvale, CA, using a JOEL 6400 FE SEM with better resolution. SEM photos by Lorenza Moro at SRI, not shown, were of targets foils of different elements [11].

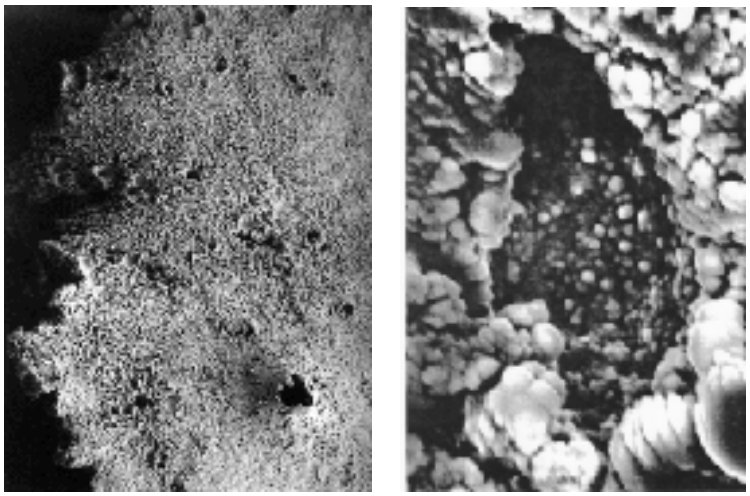

Figure 3. a SEM photo of a Pd target foil ejecta site at a frequency of 20 kHz shows the ejecta damage to the foil surface. (Maybe some high density gravitational effects) scale, 20 μm across. SEM photos 3(a) and (b), John Dash. (b) SEM photo of a detail of 3(a), a large ejecta site, in a Pd target foil exposed to 20 kHz cavitation shows one of the large multi-fusion events showing the 1μm diameter sphere debris in the vent. Woodside, CA Lab. 1993.

There is a lot more analysis work to be done with 60 exposed target foils in storage. Only a few Pd foils are shown here but the sample is a good cross section for demonstrating the differences between acoustic frequency inputs. The damage done to the target foils varies and establishes a relation between cluster size and ejecta size, number of fusion events per ejecta, and the constant energy density of these sonoluminescence systems.

Calculating the heat pulse kinetic energy of the ejected target foil mass that is vaporized, Pd heat of vaporization is 377 J/kg°C, and ejecta mass velocity for a total of about 6×10^{-12} J for a single event. The volumes of ejected target lattice atoms, numbering 3×10^{6} Pd atoms, are ejecta from a site at the resonant frequency of (C). See Fig. 5(b). The energy of one DD fusion event producing ^{4}He is about 4×10^{-12} J. The (C) cluster ejection sites of the surveyed foil surface found in a 1 μm^2 area are 30–50 nm in diameter and about equivalent to the energy of one DD helium fusion

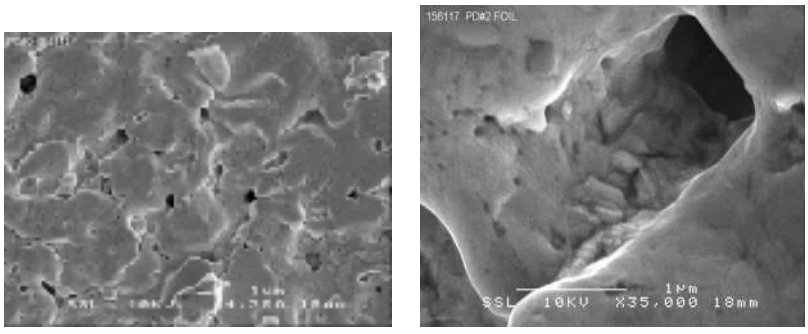

Figure 4. a) SEM photo of a Pd target foil ejecta sites at a frequency of 46 kHz shows the ejecta damage to the foil surface. Much milder damage than 20 kHz. SEM photos, Scale 1 cm = 4μm (b) Detail from 4(a) SEM photo of several square μm of 4(a) Pd target foil exposed to 46 kHz cavitation shows the diversity of the ejecta population. Scale 1 cm = 1 μm . SEM photos, Jane Wheeler, Evans Lab., Sunnyvale CA. Foil from SRI, Menlo Pk. CA.

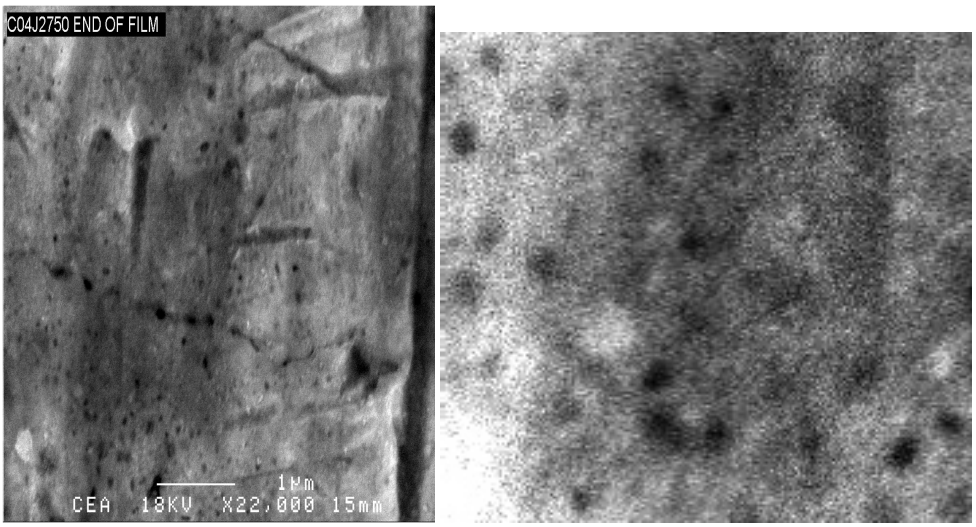

Figure 5. (a) SEM photo of a Pd target foil with ejecta sites at a frequency of 1600 kHz shows the ejecta damage to the foil surface. The damage is minimal to the exposed foil surface. Scale 1 cm = 1 μm. (b) Detail from 5(a) SEM photo of a square μm of 3e Pd target foil exposed to 1.6 kHz cavitation shows the uniformity of the ejecta population in the 50 nm diameter range. Scale 2 mm = 50 nm. Jane Wheeler, Evans Lab., Sunnyvale, CA. Foil from First Gate, Kilauea, HI.

event. (It is expected that the same results will be found in exposed target foils of other elements.) A spherical heat pulse expands through the Pd lattice until it reaches the foil surface where the heat pulse breaks the plane of the foil surface and ejects the contents of the ejecta site into the circulating D_2O at a velocity of about 3000 m/s. The fusion heat pulse starting a temperature of 10^9K expands its lattice volume spherically to 4000 K ejecta temperature. The instant the cavitation process is stopped the surface is frozen and allows for a leisurely SEM photo analysis of the foil surface. One often sees, via SEM, in the interior of the larger vent sites, 2000–10,000 nm in diameter, 1 μm and smaller diameter spheres of recondensed target foil that loosely coalesce in and on the target foil vent site surface, Fig. 2(b). The path from the jet plasma formation to the ejecta site is reasonable, but not the only path to DD fusion.

7. Discussion

Measured fusion heat and nuclear products show that a non-obvious path is necessary to explain experimental results. Calorimetry measures the excess heat, Qx. The calorimetry used was the D_2O flow through type and is described in [4]. One measures ΔT of D_2O at measured flow rate F. The Joules of heat exiting, $\Delta T \times Fx4.669 = Q_o$, are measured. The specific heat constant for D_2O of 4.669 J/(g K) is from [12]. The acoustic watts input are measured, $Q_a.Q_o - Q_a = Qx$, the excess heat in watts, DD fusion heat, and is a product along with measured ^{4}He.

The nuclear products measured by mass spectroscopy from gases collected during experiments at 20 kKHz (A) on Pd foil system by the DOE's Brian Oliver showed 452 ppm of ^{4}He in the 50 cm^3 sample volume [4,6]. Fusion products escaped the target lattice via the heat pulse ejecta into circulating D_2O where gases were collected and sampled. Also measured by mass spectroscopy were T and ^{4}He and ^{3}He from experiments with D_2O cavitation exposed Ti foil [11]. In earlier experiments in 1990, inductively coupled plasma MS measurements showed the presence of the lone isotope Cs 112 [13].

Nuclear products, gammas and/or neutrons associated with hot fusion, measured and not found. So, one must explain the measured ^{4}He production as originating in a piece of matter like a BEC cluster. Here is a dense environment

that produces ^{4}He and Qx before any other products can be formed. The result is usable energy without harmful long-range radiation.

The muon, μ, fusion of two deuterons, if thought of as a pseudo BEC, is a parallel to sonofusion. The overlap of the Boson DDμ at 10^{-12} m separation and the increasing fusion rate as the temperature is lowered, fit BEC muon fusion phenomena.

The environment of sonofusion is cavitated, Ar saturated, and reactor circulated D_2O. A target foil is carefully placed in the reactor. A cavitation produced transient deuteron cluster of BEC deuterons is implanted into the lattice, and serves as the containment for this sub-nano scale cluster. The initially dense cluster is further compressed and cooled by evaporative surface deuterons of the cluster. These interact with free electrons away from the cluster-forming deuterium atoms that surround the cluster. This leaves the cluster cooler but with fewer deuterons. These Coulombic accelerating free electrons produce an imploding spherical electromagnetic pulse that squeezes the cluster to fusion densities in less than a picosecond. These electrons are hot enough and will pass through the evaporative-formed deuteron ions to the fresh surface of the clustered deuterons to keep the implosion pulse compressing for about 0.1 ps. The compressing cluster approaches the density of muon ion DDμ^+. The fusion event initiates a heat pulse destroying the cluster. The spherical heat pulse travels into and through the lattice to the target foil surface. There it erupts with lattice ejecta, Figs. 3–5, and fusion products ^{4}He and heat are ejected into the D_2O, and measured by mass spectroscopy and calorimetry. Left behind in the target foil are ejecta sites frozen in the target foil, easily analyzed by SEM, and their ejecta size relates to the number of fusion events per site via the energy of their ejecta volume.

An interesting comparison between SF and muon fusion are its density and BEC nature. In a conversation with Steve Jones, who was historically involved in early cold fusion, regarding his muon fusion experiments stated the colder the μ bombardment of liquid deuterium the faster the fusion rate. The de Broglie wave function overlap in the DDμ^+ will increase at lower temperatures decreasing the T/T_c ratio, decreasing the amount of contact time needed per fusion event in that chain reaction. This is the case if the cluster density is 10^{36} D^+/m^3. Sonofusion may respond to the same lowering of the cluster temperature via recombination and a more favorable fusion environment.

The system of cavitating D_2O in a piezo-produced acoustic field creates cavitation bubbles as a precursor to high-density implanting plasma jets, Bose Einstein Condensate clusters, where fusion events occur. A good review of single bubble cavitation and densities produced during the collapsing bubble and other pertinent cavitation data about water bubbles in their final stages of collapse can be found in reference [4]. As the Mach 4 surface collapse of the cavitation bubble [14] terminates the bubble, an ejection of some of the collapsed bubble plasma contents compresses and dissociates D_2O, forming high density jet plasmas. The dense z pinch accelerating plasma jet is injected into the cavitating D_2O via the bubble collapse and implants into a target foil, where for a picosecond EM-squeezed and evaporated cooled BEC clusters fuse producing excess heat and ^{4}He. The BEC fusion environment has a high ion density and is superconducting. Unique properties relate to BEC cluster MeV D^+ energy levels via its nuclear shell model. The fusion heat pulse that terminates the cluster explodes from the target foil surface as ejecta carries vaporized target foil and fusion products into the D_2O. All of the above can be found in my earlier papers and in references [4,6].

It is interesting that the visually observed Pd surface of an exposed 2-mm thick target did not show the damage found in the 100 μm Pd foils. The thin Pd foils show very obvious ejecta damage and also strong induced MHz standing wave forms in the (A) and (B) resonance system, Fig. 2 [11]. If one looks at the 4000 K of the cluster, the T/T_c ratio of 0.000002 should provide a good fusion environment for BEC fusion. It is the fusion in the transient BEC clusters contained in the 100-μm thick Pd target foil that produces target foil ejecta sites.

8. Summary

The system of cavitating D_2O in a piezo produced acoustic field creates cavitation bubbles as the Mach 6 surface bubble collapse terminates with the jet and sonoluminescence, and the sequence to fusion continues. High-density lattice

implanting z-pinch plasma jets provides a picosecond separation of deuterons and electrons. The accelerating free electrons trap some deuterons in an EM pulse forming 1 nm deuteron clusters. The picosecond EM pulse overwhelms the the cluster's Coulombic repulsion squeezing deuteron Bose Einstein Condensate clusters. The pulse provides for dense and evaporative cooled environments for DD fusion events. The fusion heat, Qx, produced a heat pulse that expels fusion products of Qx and ^{4}He from the lattice. The escaping fusion heat pulse leaves SEM observable ejecta sites. This is the proposed sequential path to clean usable energy.

The normal BEC forms at ultra low temperatures because in ordinary matter, it includes electrons. The BEC exists only between the ground state and the next energy level, maybe 0.06 eV. However, in the deuteron cluster, for a picosecond, the next level above ground state is 2.32 MeV [9] as there are no electrons. The cluster EM compression pulse is stronger than the Coulombic repulsion for a picosecond. That is enough contact time for the BEC cluster fusion event to occur.

The BEC is composed of Bosons, even numbered spins (deuterium, ^{4}He, H, H_2, H_2^{2+}, etc.). Fermions have an odd numbered spin like $^1/_2$ for electrons, protons, and neutrons, where two protons may form an electron free Boson cluster. The Fermion protons may assume a Boson mode by pairing, and for a picosecond have the properties of a BEC that leads to the observed lattice ejecta effects [15]. Fermions have the ability to couple, forming bosons and may explain their damaging effects in cavitated target foils in H_2O.

Acknowledgements

I would like to thank Julie Wallace, Jim Reiker, and Dick America for their support over many years of work, and also Dennis Letts, Fran Tanzella, Steve Krivit, Joe McDowell, Joel Garbon, Jan Marwan, Scott Chubb and many others for helping to put these ideas into the mainstream.

References

[1] R.D. Petrasso et al., Proton radiography of inertial fusion implosions, *Science* **319** (2008) 1223–1225.
[2] M.A. Liberman, J.S. De Groot, A. Toor and R.B. Spielman, *Physics of High-Density Z-Pinch Plasmas*, Springer-Verlag, NY, 1998, p. 19 and pp. 238–241.
[3] T. Fukuyama and M. Morikawa, Relative BEC Model for Matter and Energy, ESO Astrophysics Symposia, *Relativistic Astrophysics and Cosmology- Einstein's Legacy*, Springer-Verlag, NY, 2007, p. 96.
[4] R.S. Stringham, *Sonofusion, Deuterons to Helium Experiments,* ACS, LENR sourcebook, Vol. 2, Jan Marwan and Steve Krivit (ed.), 2009.
[5] Y. Tomita and A. Shima, High speed photographic observations of laser induced cavitation bubbles in water, *Acoustica* **71** (1990) 161. M.P. Felix and A.T. Ellis, Laser-induced liquid breakdown – a step by step account, *Appl. Phys. Lett.* **19** (1971) 484. W. Lautterborn and J. Bolle, Experimental investigations of cavitation- bubble collapse in the neighborhood of a solid boundary, *Fluid Mech.* **723** (1975) 91.
[6] R.S. Stringham, *Model for Sonofusion*, AIP Conference Proc., San Francisco, CA, LENR, Jan Marwan (ed.), 20–21 March 2010, To be published.
[7] M.P. Brenner, S. Hilgenfeldt and D. Lohse, Single bubble sonoluminescence, *Rev. Modern Phys.* **74**(2) (2002) 425–484.
[8] N.D. Cook, *ICCF-15 Proceedings*, Poster, V. Violante (ed.), Rome, Italy, 2009, to be published.
[9] M. Ragheb, *Deuteron Disintegration in Condensed Matter,* 2007, https://netfiles.uiuc.edu/mragheb/www/NPRE%20402%20ME%20405%20Nuclear%20Power%20Engineering/Deuteron%20disintegration%20in%20condensed%20matter.pdf
[10] S. Badiei, P.U. Andersson and L. Holmlid, Production of ultradense deuterium: A compact future fusion fuel, *Appl. Phys. Lett.* **96** (2010) 96, 124103-1
[11] R.S. Stringham, *ICCF-15 Proceedings*, Poster, V. Violante (ed.), Rome, Italy, 2009, to be published.
[12] M. Nakamura, K. Tamura, S. Murakami, Isotope effects on thermodynamic properties: mixtures of x(D_2O *or* H_2 O) + (1 - x)CH_3 CN at 298.15 K, *Thermochi. Acta* **253** (1995) 127–136.

[13] R.S. Stringham, Fusion product analysis – ICP of Pd 108 ◇ Cs 112 by Samantha Tam, Balazs Laboratories, Sunnyvale, CA (1990). No other Cesium isotopes detected.
[14] K.R. Weninger, P.G. Evans and S.J. Putterman, Time correlated single photon Mie scattering from a sonoluminescing bubble, *Phys. Rev.* E **61**(2) (2000) 1020.
[15] Y. Kim, Theory of BEC mechanism for deuteron-induced nuclear reactions in micro/Nano-scale metal grains and particles, *Naturwissenschaften* **96** (2009) 803–811.